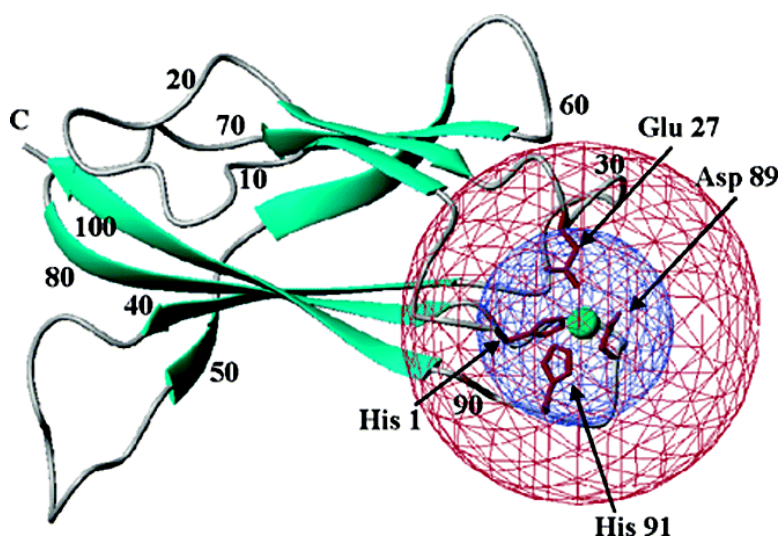# JACS
JOURNAL OF THE AMERICAN CHEMICAL SOCIETY

Article

A Strategy for the NMR Characterization of Type II Copper(II) Proteins: the Case of the Copper Trafficking Protein CopC from *Pseudomonas Syringae*

Fabio Arnesano, Lucia Banci, Ivano Bertini, Isabella C. Felli, Claudio Luchinat, and Andrew R. Thompsett

More About This Article

Additional resources and features associated with this article are available within the HTML version:

- Supporting Information
- Links to the 6 articles that cite this article, as of the time of this article download
- Access to high resolution figures
- Links to articles and content related to this article
- Copyright permission to reproduce figures and/or text from this article

View the Full Text HTML

A Strategy for the NMR Characterization of Type II Copper(II) Proteins: the Case of the Copper Trafficking Protein CopC from *Pseudomonas Syringae*

Fabio Arnesano,[†,‡] Lucia Banci,[†,‡] Ivano Bertini,*[,†,‡] Isabella C. Felli,[†,‡] Claudio Luchinat,[†,§] and Andrew R. Thompsett[†,‡]

Contribution from the CERM, University of Florence, Via Luigi Sacconi 6, 50019 Sesto Fiorentino, Florence, Italy, Department of Chemistry, University of Florence, Via della Lastruccia 5, 50019 Sesto Fiorentino, Florence Italy, and Department of Agricultural Biotechnology, University of Florence, P.le delle Cascine 28, 50144 Florence, Italy

Received January 10, 2003; E-mail: bertini@cerm.unifi.it

Abstract: CopC from *Pseudomonas syringae* was found to be a protein capable of binding both Cu(I) and Cu(II) at two different sites. The solution structure of the apo protein is available, and structural information has been obtained on the Cu(I) bound form. We attempt here to set the limits for the determination of the solution structure of a Cu(II) protein, such as the Cu(II) bound form of CopC, in which the Cu(II) ion takes a type II coordination. The electron relaxation time is estimated from NMRD measurements to be 3 ns which leads to a correlation time for the nuclear spin−electron spin dipolar interaction of 2 ns. This information allowed us to tailor the NMR experiments and to fully exploit purely heteronuclear spectroscopy to assign as many signals as possible. In this way, 37 ^{13}C and 11 ^{15}N signals that completely escape detection with conventional approaches were assigned. Paramagnetic based structural constraints were obtained by measuring paramagnetic longitudinal relaxation enhancements (ρ^{para}) which allowed us to precisely locate the copper ion within the protein frame. Pseudocontact shifts (pcs's) were also used as constraints for 83 ^{1}H and 18 ^{13}C nuclei. With them, together with other standard structural constraints, a structure is obtained (and submitted to PDB) where information is only missing in a sphere with a 6 Å radius from the copper ion. If we borrow information from EXAFS data, which show evidence of two copper coordinated histidines, then His 1 and His 91 are unambiguously identified as copper ligands. EXAFS data indicate two more light donor atoms (O/N) which could be from Asp 27 and Glu 89, whereas the NMRD data indicate the presence of a semicoordinated water molecule at 2.8 Å (Cu−O distance) roughly orthogonal to the plane identified by the other four ligands. This represents the most extensively characterized structure of a type II Cu(II) protein obtained employing the most advanced NMR methods and with the aid of EXAFS data. The knowledge of the location of the Cu(II) in the protein is important for the copper transfer mechanism.

Introduction

Copper proteins are quite common, as copper is an essential and abundant element.[1−3] Often copper is present in the cellular media as Cu(I), although Cu(II) is also present. The NMR characterization of Cu(II) proteins represents a challenge, as Cu-(II) has long electron relaxation times and the NMR signals of nuclei in the vicinity of the metal ion may be broadened beyond detection.[4,5]

Among copper proteins, a distinction should be made between proteins containing type I and type II copper with respect to their NMR properties. Proteins bearing type I copper always contain a cysteine and are characterized by a low coordination number, that is, three- or four-coordinated. Both features are responsible for the electronic relaxation times of Cu(II) being in the low range (0.2−0.8 ns) of the values found for Cu(II) complexes.[5−7] The study of type I copper-containing proteins by NMR was pioneered by Canters et al.,[8] and our lab succeeded in solving the first solution structure for one such protein where all the protons of all the ligands were assigned and used as sources of structural information.[9]

† CERM, University of Florence.
‡ Department of Chemistry, University of Florence.
§ Department of Agricultural Biotechnology, University of Florence.

(1) Bertini, I.; Sigel, A.; Sigel, H. *Handbook on Metalloproteins*; Marcel Dekker: New York, 2001; pp 1−1800.
(2) *Handbook of Metalloproteins*; Wiley: Chichester, U.K., 2001; pp 1−1248.
(3) Frausto da Silva, J. J. R.; Williams, R. J. P. *The biological chemistry of the elements: the inorganic chemistry of life*; Oxford University Press: New York, 2001.
(4) Banci, L.; Bertini, I.; Luchinat, C. *Nuclear and electron relaxation. The magnetic nucleus-unpaired electron coupling in solution*; VCH: Weinheim, Germany, 1991.
(5) Bertini, I.; Luchinat, C.; Parigi, G. *Solution NMR of Paramagnetic Molecules*; Elsevier: Amsterdam, 2001.

(6) Koenig, S. H.; Brown, R. D., III. *Prog. Nucl. Magn. Reson. Spectrosc.* **1991**, *22*, 487−567.
(7) Kroes, S. J.; Salgado, J.; Parigi, G.; Luchinat, C.; Canters, G. W. *JBIC, J. Biol. Inorg. Chem.* **1996**, *1*, 551−559.
(8) Canters, G. W.; Hill, H. A. O.; Kitchen, N. A.; Adman, E. T. *Eur. J. Biochem.* **1984**, *138*, 141−152.
(9) Bertini, I.; Ciurli, S.; Dikiy, A.; Fernández, C. O.; Luchinat, C.; Safarov, N.; Shumilin, S.; Vila, A. J. *J. Am. Chem. Soc.* **2001**, *123*, 2405−2413.

In proteins containing type II copper, the electronic relaxation times of the metal ion are about 1 order of magnitude larger, with dramatic effects on line broadening. Therefore, the detection and assignment of signals in the vicinity of the metal ion is unexplored and likely impossible. For completeness, one should mention type III copper proteins, where two Cu(II) ions are antiferromagnetically coupled. Such coupling decreases the overall magnetic susceptibility and decreases the electronic relaxation times,[10−12] both effects leading to a decrease in line widths and to a much better detectability of the NMR lines.[13,14]

In this paper, we want to report the strategy we have developed for the NMR characterization of a type II Cu(II) protein. The pool of most suitable experiments and their optimization as well as their synergistic information are discussed with respect to the information which can be obtained. These experiments were applied to Cu(II)-CopC from *Pseudomonas syringae*, a periplasmic protein involved in copper trafficking and homeostasis in Gram-negative bacteria.[15,16] Bacteria exert resistance upon exposure to high copper levels[15−17] through a pool of proteins encoded in the cop operon, originally discovered in strains of *Pseudomonas syringae* grown in Californian tomato fields exposed to high levels of copper compounds.[18] Later the cop operon has been located in a number of other bacteria.[19] The Cop proteins are able to sequester copper ions in the periplasm and to export the excess without preventing the amount of copper essential for cellular function from reaching the cytoplasm. Key to this ability is the bifunctional protein CopC, having the intriguing property of binding Cu(I) and Cu(II) at two different sites that are 30 Å apart.[20] The apo[19] and Cu(I)[20] structures of CopC from *Pseudomonas syringae* have already been solved, but no structural information is available for Cu(II)-CopC, due to broadening of NMR signals of an extensive region of the protein around the Cu(II) binding site which prevents the use of standard techniques.

A detailed analysis of the electronic relaxation time has now allowed us to appropriately exploit the NMR technology with the aim of obtaining the best structural characterization in solution of Cu(II)-CopC.

Experimental Section

Sample Preparation. CopC was overexpressed and purified from the construct pAT2 in the *E. coli* strain BL21 (DE3) pLysS as previously described.[19] NMR samples were prepared in 100 mM sodium phosphate buffer, pH 7, containing 10% D_2O, with a protein concentration of about 2−3 mM. Binding of Cu(II) to apoCopC was followed through electronic and NMR spectroscopy as previously described.[19]

NMR Experiments. NMR experiments were carried out on a Bruker Avance spectrometer operating at a 700 MHz ^1H frequency, using a TXI probehead. All experiments were performed at 298 K. D_2O (10%) was added for the lock signal.

Saturation recovery (SR)-1D experiments were performed by saturating the ^{13}C signals using adiabatic chirp pulses[21,22] (total sweep width of 60 kHz, 1.5 ms length, $\gamma B_1/2\pi = 1.5$ kHz) in the p5m4 supercycle for 100 ms, with the ^{13}C carrier at 110 ppm. Several experiments, with different recovery delays were recorded. An appropriate linear combination of two experiments recorded with different recovery delays (see the following) was then used to identify fast relaxing signals. The remaining parameters were a 211 ms acquisition time with 16k points and 8, 16, 32, and 128 ms recovery delays. The number of scans was increased with decreasing recovery delay to ensure the detectability of weak signals (64k, 32k, 8k, and 2k scans for the experiments with recovery delays of 8, 16, 32, and 128 ms, respectively). Decoupling during acquisition was applied to ^1H (Waltz16, $\gamma B_1/2\pi = 3.3$ kHz, carrier at 4.7 ppm) and ^{15}N (garp64, $\gamma B_1/2\pi = 1$ kHz, carrier at 120 ppm).

$^{13}C-^{13}C$ constant time (CT)-COSY experiments[23,24] were acquired with the following parameters: 4096 × 320 data points, 320 scans per increment, 220 ppm spectral width in both dimensions, 52.9 ms acquisition time. The constant time (CT) delay was set to 8.3 ms. The 180° pulse present in the CT-COSY experiment was applied with an adiabatic chirp shape (total sweep width of 60 kHz, 0.5 ms length, $\gamma B_1/2\pi = 10$ kHz). The remaining pulses were hard pulses. The carrier was set to 110 ppm. The remaining parameters were the same as previously mentioned. An additional experiment was acquired centered on the $C_\alpha-C_\beta$ region with a spectral width of 80 ppm (2048 × 128 data points, 256 scans, 72 ms acquisition time) and a CT delay of 14.3 ms. The carrier was set to 50 ppm. In this case, the 180° pulse was selective on the aliphatic region (Q3 shape, 256 μs length) in order to refocus the CαCO coupling.

$^{13}C-^{15}N$ correlation experiments were acquired using carbon detection with the following parameters: recycle delay of 600 ms, acquisition of 100 ms using 512 data points and 113 increments, 1024 scans. The INEPT transfer delay was set to 25 ms.

$^{13}C-^{13}C$ and $^{13}C-^{15}N$ 2D spectra of apoCopC analogous to those described for Cu(II)-CopC were also recorded and were assigned by comparison with the 3D backbone tracing experiments and 3D HCCH-TOCSY.[19]

$^{13}C-^{13}C$ CT-COSY experiments were used to determine ^{13}C T_1's by inserting a saturation $-\tau$ building block prior to the CT COSY pulse scheme. The parameters used to saturate all ^{13}C signals are those described previously for 1D experiments. Two series of experiments were acquired, one optimized to detect Cα and Cβ signals of AMX side chains and one to detect Cα and CO backbone signals. In the Cα/Cβ series, the recovery delays were 0.1, 0.15, 0.2, 0.3, 0.5, and 1 s. In the Cα/CO series, they were 0.1, 0.2, 0.3, 0.4, 0.5, 1, and 2 s. The intensities of cross-peaks versus recovery delays (τ) were fit to the following relationship:

$$I(\tau) = A(1 - \exp(-\tau/T_1))$$

where A and T_1 are the fitting parameters.

$^1H-^{15}N$ HSQC experiments and NOESY maps (2D and 3D ^{13}C and ^{15}N edited) were acquired and processed as described for the apo form.[19]

Structure Calculations. Structure calculations were performed through iterative cycles of PSEUDODYANA[25] which uses a routine implemented to include pseudocontact shift (pcs) constraints in the structure calculations. The 35 conformers with the lowest target function

(10) Banci, L.; Bertini, I.; Luchinat, C. *Struct. Bonding* **1990**, *72*, 113−135.
(11) Clementi, V.; Luchinat, C. *Acc. Chem. Res.* **1998**, *31*, 351−361.
(12) Murthy, N. N.; Karlin, K. D.; Bertini, I.; Luchinat, C. *J. Am. Chem. Soc.* **1997**, *119*, 2156−2162.
(13) Holz, R. C.; Bennet, B.; Chen, G. J.; Ming, L. J. *J. Am. Chem. Soc.* **1998**, *120*, 6329−6335.
(14) Salgado, J.; Warmerdam, G.; Bubacco, L.; Canters, G. W. *Biochemistry* **1998**, *37*, 7378−7389.
(15) Cooksey, D. A. *FEMS Microbiol. Rev.* **1994**, *14*, 381−386.
(16) Silver, S. *Gene* **1996**, *179*, 9−19.
(17) Odermatt, A.; Suter, H.; Krapf, R.; Solioz, M. *Ann. N.Y. Acad. Sci.* **1992**, *671*, 484−486.
(18) Cha, J. S.; Cooksey, D. A. *Proc. Natl. Acad. Sci. U.S.A.* **1991**, *88*, 8915−8919.
(19) Arnesano, F.; Banci, L.; Bertini, I.; Thompsett, A. R. *Structure* **2002**, *10*, 1337−1347.
(20) Arnesano, F.; Banci, L.; Bertini, I.; Mangani, S.; Thompsett, A. R. *Proc. Natl. Acad. Sci. U.S.A.* **2003**, *100*, 3814−3819.

(21) Basus, V. J.; Ellis, P. D.; Hill, H. D. W.; Waugh, J. S. *J. Magn. Reson.* **1979**, *35*, 19−37.
(22) Riqiang, F.; Bodenhausen, G. *Chem. Phys. Lett.* **1995**, *245*, 415−420.
(23) Bax, A.; Freeman, R. *J. Magn. Reson.* **1981**, *44*, 542−561.
(24) Rance, M.; Wagner, G.; Sorensen, O. W.; Wüthrich, K.; Ernst, R. R. *J. Magn. Reson.* **1984**, *59*, 250−261.
(25) Banci, L.; Bertini, I.; Cremonini, M. A.; Gori Savellini, G.; Luchinat, C.; Wüthrich, K.; Güntert, P. *J. Biomol. NMR* **1998**, *12*, 553−557.

constituted the final family. Structure calculations were run on a Linux processor cluster. Structure analysis was performed with the PROCHECK NMR program.[26]

NMRD Experiments. Longitudinal water proton relaxation rates were measured with a Koenig–Brown field cycling relaxometer (0.01–50 MHz proton Larmor frequency range) and a Stelar fast field cycling relaxometer (0.01–20 MHz proton Larmor frequency range) as a function of the magnetic field. Both instruments provide water proton R_1 values with an error of about 1%.

From the experimental relaxation rates, the diamagnetic contribution to these rates, as evaluated from the apo form, was subtracted and the resulting values scaled to the mM concentration of copper. These latter values are called relaxivity and were fitted according to the reported analysis.[5,27,28]

Results

Electronic Relaxation Time of Cu(II)-CopC. Nuclear longitudinal (R_1) and transverse (R_2) relaxation rates, due to the coupling with a paramagnetic center, are strongly dependent on the electronic relaxation time according to the Solomon–Bloembergen equations:

$$R_{1M} = \frac{2}{15}\left(\frac{\mu_0}{4\pi}\right)^2 \frac{\gamma_I^2 g_e^2 \mu_B^2 S(S+1)}{r^6}\left[\frac{\tau_c}{1+(\omega_I-\omega_S)^2\tau_c^2}+\right.$$
$$\left.\frac{3\tau_c}{1+\omega_I^2\tau_c^2}+\frac{6\tau_c}{1+(\omega_I+\omega_S)^2\tau_c^2}\right]+\frac{2}{3}S(S+1)$$
$$\left(\frac{A}{\hbar}\right)^2\frac{\tau_e}{1+\omega_S^2\tau_e^2} \quad (1)$$

$$R_{2M} = \frac{1}{15}\left(\frac{\mu_0}{4\pi}\right)^2 \frac{\gamma_I^2 g_e^2 \mu_B^2 S(S+1)}{r^6}\left[4\tau_c+\right.$$
$$\frac{\tau_c}{1+(\omega_I-\omega_S)^2\tau_c^2}+\frac{3\tau_c}{1+\omega_I^2\tau_c^2}+\frac{6\tau_c}{1+(\omega_I+\omega_S)^2\tau_c^2}+$$
$$\left.\frac{6\tau_c}{1+\omega_S^2\tau_c^2}\right]+\frac{1}{3}S(S+1)\left(\frac{A}{\hbar}\right)^2\left(\tau_e+\frac{\tau_e}{1+\omega_S^2\tau_e^2}\right) \quad (2)$$

where the first term of each equation describes the contribution from the electron spin–nuclear spin dipolar interaction, which depends on the reciprocal sixth power of the electron–nucleus distance and the second term describes the Fermi contact contributions, which depend on the fraction of unpaired electrons delocalized through chemical bonds onto the resonating nucleus. γ_I is the nuclear gyromagnetic ratio, g_e is the free electron g factor, S is the quantum number associated to the electron spin, r is the electron–nucleus distance, ω_I and ω_S are the Larmor frequencies of the nucleus and of the electron, respectively, τ_e is the electronic correlation time, τ_r the rotational correlation time and τ_c is the effective correlation time for the dipole–dipole interaction ($1/\tau_c = 1/\tau_e + 1/\tau_r$), A_c is the constant for the contact coupling between the electron spin and the nuclear spin, and the remaining symbols have their usual meaning. These equations were appropriately modified for slow rotating systems, such as proteins, to account for the presence of the hyperfine
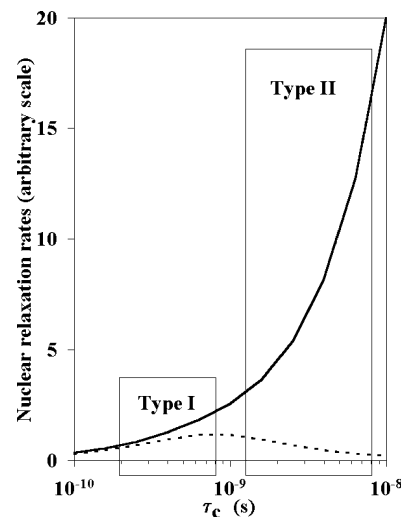
(26) Laskowski, R. A.; Rullmann, J. A. C.; MacArthur, M. W.; Kaptein, R.; Thornton, J. M. *J. Biomol. NMR* **1996**, *8*, 477–486.
(27) Bertini, I.; Briganti, F.; Luchinat, C.; Mancini, M.; Spina, G. *J. Magn. Reson.* **1985**, *63*, 41–55.
(28) Bertini, I.; Galas, O.; Luchinat, C.; Parigi, G. *J. Magn. Reson. Ser. A* **1995**, *113*, 151–158.

Figure 1. Plot of the theoretical electron–nucleus dipole–dipole contribution to longitudinal (dotted line) and transverse (continuous line) relaxation rates as a function of τ_c.
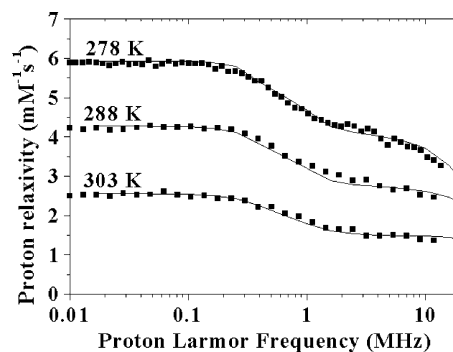

Figure 2. Water proton relaxivity of Cu(II)-CopC solutions obtained at three different temperatures. Data were fitted with two protons at 3.5 Å, $A_{||}$ = 0.0177 cm^{-1}, $A_\perp$ = 0 cm^{-1}, and Θ = 42°. τ_s ranges from 1 × 10^{-9} s (278 K) to 2 × 10^{-9} s (303 K).

coupling with the $I = {}^3/_2$ copper nucleus and of g-tensor anisotropy,[27,28] and computer programs were developed to fit experimental data. For medium-sized proteins and in the absence of very fast exchange phenomena, the correlation times for both processes, that is, dipolar and contact, are dominated by the electronic relaxation time τ_s. The dependence of nuclear R_1 and R_2 values on the electronic relaxation time at high magnetic field (Figure 1) shows that, in type II copper proteins, in addition to a more dramatic line broadening than in type I copper proteins, also a decrease of the longitudinal relaxation rate occurs, thus preventing the use of very fast recycle times. To devise the best experimental strategy for high resolution NMR on a type II copper protein, a good estimate of the electronic relaxation time is obviously required. Such an estimate can be obtained from the water proton longitudinal relaxation enhancement as a function of magnetic field (nuclear magnetic relaxation dispersion, NMRD). If the solvent molecules interact with the Cu(II) ion in the protein and they exchange fast with the bulk ones, the water proton nuclear R_1 contains a contribution due to the dipolar interaction with the copper unpaired electron. The NMRD profiles of a solution of copper(II)-CopC at three different temperatures are shown in Figure 2, together with their best fits to eq 1 and its modifications.[5,27,28] The relevant information obtained from this analysis is the value of τ_s and the metal–proton distance assuming the interaction arises mainly

from one water molecule (see later). τ_s has a value of 3 ns at room temperature which, together with the value of τ_r of 6 ns estimated from ^{15}N relaxation data,[19] yields a correlation time τ_c of 2 ns for the dipolar part of the electron−nucleus interaction, while the value of τ_s by itself yields the correlation time for the Fermi contact part of the interaction.

High-Resolution NMR of CopC. As already reported,[19] binding of Cu(II) to the protein produces dramatic effects on the NMR spectra. From the analysis of the electron relaxation properties of Cu(II) in CopC and from the theoretical prediction (Figure 1), a nuclear R_2/R_1 ratio of about 5 is expected for all protein nuclei experiencing dipole−dipole coupling with the unpaired electron. When standard experiments based on ^{1}H detection are performed, resonances of 18 residues are not detected, which are located within about 11 Å from the potential copper binding site.[19] Another set of signals from residues in the borderline region are still detectable in standard spectra acquired on Cu(II)-CopC, but they experience variable broadening and/or differences in chemical shift with respect to the corresponding ones in the apo protein. The rest of the signals of Cu(II)-CopC have essentially the same shift as in the spectra of apoCopC. Signal assignment and structural constraints for the latter set of signals, belonging to residues far from the Cu-(II) binding site, are obtained with the standard procedures, also taking into account the results available for the apo protein.[19] Also the set of residues that experience a shift upon Cu(II) binding but that are still detectable in the standard HSQC spectra can easily be assigned through ^{13}C- and ^{15}N-edited NOESY-HSQC experiments, which provided NOE cross-peaks of about 10 borderline residues. A further attempt has been made using mixing and repetition times optimized according to the R_2/R_1 ratio and a few additional connectivities could be detected. In total, 1777 unique upper distance limits were obtained from the assigned NOE cross-peaks, involving about 80% of the protons. Still, 5 residues remained partly undetected and 13 residues totally undetected. A limit for the NMR investigation of this system is due to the combination of extensive line broadening and lack of large hyperfine shifts: detectability of broad NOESY cross-peaks in spectral regions crowded by sharp peaks is intrinsically unfavorable.

Detection of Fast Relaxing Heteronuclei. To extend the assignment in the closer proximity of the paramagnetic center, we have therefore chosen experiments based on heteronuclei, because of their lower magnetogyric ratio (γ) compared to protons and thus they are less affected by dipole−dipole contributions to relaxation that depend on γ^2 (eqs 1 and 2). If only dipole−dipole relaxation is considered, the paramagnetic broadening with respect to protons for the same metal−nucleus distance is reduced about 16-fold for ^{13}C nuclei and about 100-fold for ^{15}N nuclei.[51] This means that the radius of the blind sphere should decrease from about 11 Å for protons to about 7 Å for carbons and to 5 Å for nitrogens.

Recently, direct ^{13}C−^{13}C [29,30] and ^{13}C−^{15}N [31] experiments not involving protons and using direct detection of ^{13}C have been proposed for paramagnetic proteins. Despite the reduced
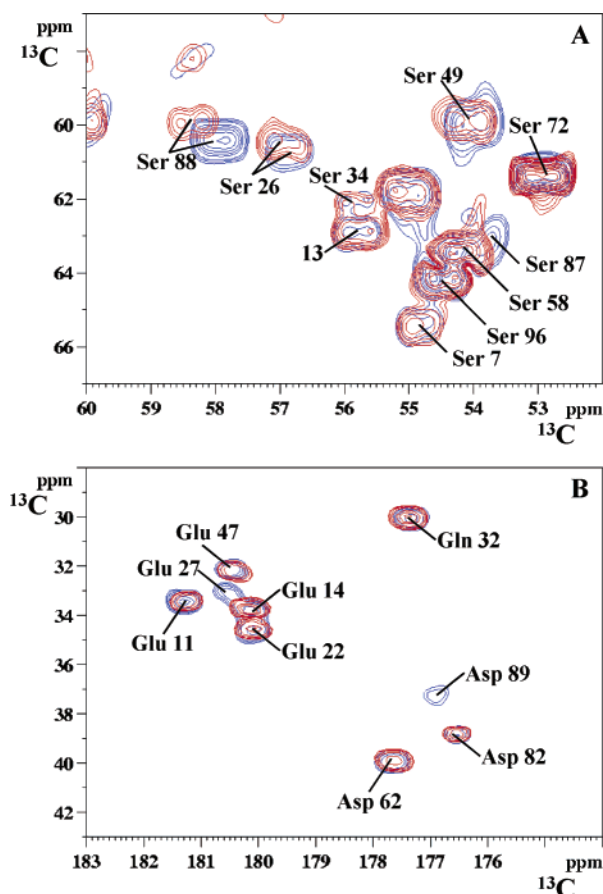
(29) Bertini, I.; Lee, Y.-M.; Luchinat, C.; Piccioli, M.; Poggi, L. *ChemBioChem* **2001**, *2*, 550−558.
(30) Machonkin, T. E.; Westler, W. M.; Markley, J. L. *J. Am. Chem. Soc.* **2002**, *124*, 3204−3205.
(31) Kostic, M.; Pochapsky, S. S.; Pochapsky, T. C. *J. Am. Chem. Soc.* **2002**, *124*, 9054−9055.

Figure 3. Two regions of ^{13}C−^{13}C CT-COSY spectra showing (A) Cα−Cβ connectivities of serines (taken from the spectrum optimized to detect Cα−Cβ connectivities in AMX systems) and (B) side chain C−CO connectivities (taken from the spectrum optimized to detect Cα−CO connectivities which also yields side chain C−CO connectivities of Asp, Asn, Glu, and Gln). Blue and red contours refer to the apo and to the Cu-(II) bound forms, respectively.

sensitivity with respect to standard proton-detected experiments and the smaller heteronuclear−heteronuclear ^1J couplings involved ($^1J_{CC}$ 35−55 Hz, $^1J_{CN}$ ∼15 Hz) with respect to the proton−heteronuclear counterparts ($^1J_{HC}$ ∼150 Hz, $^1J_{HN}$ ∼90 Hz), the paramagnetic R_2 enhancement is so much smaller that cross-peaks should be detected at sizably closer metal−nucleus distances.

On our system, we decided to acquire two ^{13}C−^{13}C CT-COSY experiments, which detect intraresidue C−C connectivities, with different CT delays, one optimized to detect Cα−CO backbone connectivities (CT delay of 8.3 ms) and one to detect Cα−Cβ connectivities (CT delay of 14.2 ms) of AMX spin systems. The experiment optimized for Cα−CO connectivities takes advantage of the shorter CT delay, minimizing relaxation losses, and the fact that all connectivities can be in principle observed, although at the expense of resolution in the indirect dimension and of sensitivity in some types of connectivities depending on the spin topology. For this reason, the second experiment was also acquired with improved sensitivity for Cα−Cβ connectivities in AMX spin systems (Figure 3A).

^{13}C−^{15}N HSQC spectra[32] were used to detect sequential correlations between the backbone ^{13}CO resonance of residue i and the amide ^{15}N of residue $i + 1$. Also in this case, and at

(32) Bodenhausen, G.; Ruben, D. J. *Chem. Phys. Lett.* **1980**, *69*, 185−188.
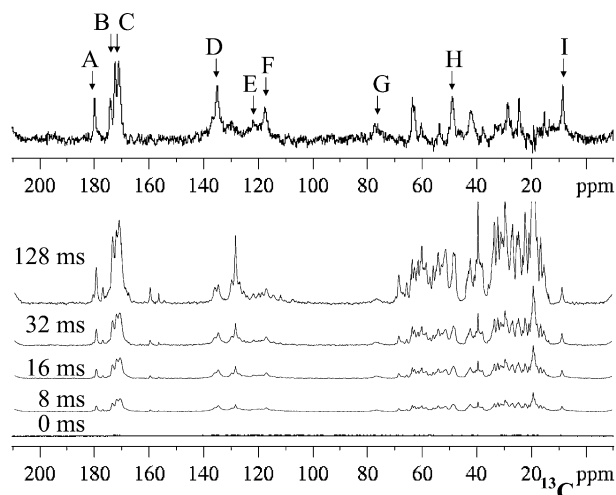
Figure 4. Saturation recovery (SR) 1D ^{13}C spectra with different recovery delays (0, 8, 16, 32, 128 ms) are reported in the lower part of the figure. Experiments with shorter recovery delays were acquired with an increasing number of scans to maintain a good signal-to-noise ratio (64k, 32k, 8k, and 2k scans for the experiments with recovery delays of 8, 16, 32, and 128 ms, respectively). The spectra are rescaled according to the number of scans to have comparable signal intensities. A difference spectrum between the experiments with 32 and 128 ms recovery delays is also shown in the top. The broad signals that can be identified in the difference spectrum are labeled.

Table 1. ρ^{para} (Hz) and Upper (UPL) and Lower (LOL) Distance Constraints (Å) between the Listed Nuclei and the Copper Ion Used in the Structure Calculations of Cu(II)-CopC

	atom		ρ^{para} (Hz)	UPL	LOL
6	SER	CO	0.3	14.8	12.1
25	PHE	CO	1.1	12.0	9.8
29	LEU	CO	0.48	13.8	11.3
30	VAL	CO	0.57	13.4	10.9
31	THR	CO	0.11	17.7	14.5
32	GLN	CO	0.28	15.1	12.4
33	PHE	CO	0.21	15.8	12.9
84	ARG	CO	0.34	14.6	12.0
85	ALA	CO	3.70	9.8	8.0
93	ILE	CO	1.67	11.2	9.2
94	THR	CO	0.27	15.2	12.4
6	SER	Cα	0.21	15.8	12.9
26	SER	Cα	0.74	12.8	10.9
29	LEU	Cα	0.88	12.5	10.2
30	VAL	Cα	0.27	15.2	12.4
31	THR	Cα	0.18	16.3	13.3
32	GLN	Cα	0.36	14.5	11.8
84	ARG	Cα	0.38	14.4	11.7
85	ALA	Cα	1.02	12.2	9.9
88	SER	Cα	3.70	9.8	8.1
93	ILE	Cα	4.89	9.4	7.7
93	ILE	Cδ$_1$	4.89	7.5	5.5
94	THR	Cα	0.65	13.1	10.7

variance with the previous application to a nickel(II)-containing protein,[31] the acquisition parameters were optimized to minimize relaxation losses and still retain a suitable resolution.

With the previous experiments, new ^{13}C resonances, not detected in standard experiments, are identified, but several ^{13}C signals still escape detection because their broad and weak cross-peaks lie underneath a crowded region of sharp and intense cross-peaks. Therefore, several SR-1D ^{13}C experiments were collected with different recovery delays with the aim of identifying ^{13}C peaks characterized by short R_1 values. The detection of these signals dramatically depends on the level of ^{13}C signal saturation which with our method (see experimental part) was excellent as shown by the lowest trace in Figure 4. 1D spectra obtained with increasing recovery delays (16, 32, 64, and 128 ms) clearly show a small number of signals that recover much faster than all the others (Figure 4). The selectivity of these experiments can be further improved by an appropriate linear combination of two SR-1D experiments recorded with different recovery delays. In this way, it is possible to further suppress slower relaxing signals, whose recovery profile should be linear for short recovery delays (short compared to their T_1 values), and better highlight paramagnetic signals, whose recovery profile deviates from linearity. The appropriate linear combination can be achieved either by using two processed spectra acquired separately or by direct acquisition of difference experiments. In this way, nine signals close to the paramagnetic center could be detected. These nine resonances can be subdivided in two classes characterized by different relaxation behavior and different R_2/R_1 ratios, one with a ratio close to 5, which is expected for pure dipolar contribution to relaxation, and the other with larger ratios, which can be taken as an indication of an additional Fermi contact contribution to R_2. Therefore, signals of the latter class (as an example signal G of Figure 4) must be connected to the paramagnetic center through covalent bonds.

The simultaneous availability of ^{13}C$-^{13}$C and ^{13}C$-^{15}$N connectivities allowed the sequential assignment of most of the newly detected, paramagnetically perturbed, heteronuclear signals. The easily available analogous data for apoCopC were then used to support this assignment. Therefore, the combination of ^{13}C$-^{13}$C and ^{13}C$-^{15}$N 2D connectivities appears a general tool to extend the assignment of paramagnetic proteins significantly closer to the metal center. The nine paramagnetic signals detected in the SR-1D spectra did not show a recognizable cross-peak in the 2D ^{13}C$-^{13}$C experiments, and their assignment is not univocal (except for one isolated signal).

Overall, 37 ^{13}C and 11 ^{15}N new resonances that escaped detection with conventional methods involving ^{1}H, even if optimized for fast relaxing signals, could be detected and assigned.

The results of the assignment are summarized in Table 1 of the Supporting Information. In total, about 85% of carbon atoms and 95% of nitrogen atoms can be assigned, representing a substantial increase with respect to the standard approach (76% and 83%, respectively). More importantly, extensive heteronuclear assignment is now available for 15 additional residues, 10 of which had totally escaped detection. Only three residues are still totally unassigned. These are His 1, Asp 89, and His 91. These residues are thus obvious candidates as copper donors in CopC (see later).

Heteronuclear Paramagnetism-Based Constraints and Structure Calculations. Translating new heteronuclear assignments into new constraints is not, however, a trivial task. Heteronuclear chemical shifts can provide structural constraints through CSI. However, in a paramagnetic system, pseudocontact shifts (pcs's) are also present: in the case of modest magnetic susceptibility anisotropy, such as for Cu(II) ions, the expected pcs's are of the order of the spreading of chemical shifts for a particular heteronucleus, and the two effects are therefore difficult to separate as an appropriate diamagnetic blank has to be available. In the present case, the apoCopC may not constitute a reliable blank as the conformational changes occurring upon

binding of Cu(II) can affect the diamagnetic shift of heteronuclei. As heteronuclear CSI and/or pcs values would constitute precious structural constraints, we separate them by estimating the pseudocontact shift through their iterative fitting with the structure calculation. The axial magnetic susceptibility anisotropy can be initially estimated from the $g_{\parallel}$ value measured in the EPR spectra[19,33] which do not show appreciable rhombicity, allowing us to set an upper limit of the rhombic magnetic anisotropy to be about 10% of the axial term, while the tensor orientation can be initially estimated from proton pseudocontact shifts as proton shifts are less sensitive than heteronuclear shifts to conformational changes. Furthermore, only protons relatively far from the metal can be detected, so they are less likely involved in conformational changes in passing from the apo to the metal bound state. Nonnegligible pcs values for 83 protons could be confidently measured by subtracting the shift of the corresponding proton in apoCopC.

Another type of very useful structural constraint available in paramagnetic systems is the relaxation rate enhancement. Several examples have appeared in which ^{1}H longitudinal relaxation rate enhancements (ρ^{para}) were used as structural constraints.[34-37] At variance with transverse relaxation rates, longitudinal relaxation rates in a Cu(II)-containing protein are only sensitive to the dipole−dipole part of the interaction (first term of eq 1) and therefore can be safely used as structural constraints even for those nuclei that may experience unpaired spin delocalization. Finally, better results are expected for ^{13}C than ^{15}N nuclei; as for the latter, the low gyromagnetic ratio is expected to make the paramagnetic contribution to longitudinal relaxation negligible already at relatively short distances from the metal.

The most sensitive ^{13}C experiments (1D and 2D ^{13}C CT COSY) have been modified to measure longitudinal ^{13}C relaxation rates. A saturation block, followed by a delay τ, was inserted prior to the beginning of the experiment, and several experiments were recorded with different values of τ, in a SR scheme. This scheme was preferred to the inversion recovery method because the longer ^{13}C rates, if compared to protons, would require a longer recycle delay to ensure that magnetization has fully relaxed to equilibrium before starting the next transient. Indeed with our approach, the complete set of experiments could be acquired in a reasonable amount of time (4.5 days on a 700 MHz). As an example of the quality of the data, two SR profiles are shown in Figure 5, one representing a fast relaxing signal, the other, a slow relaxing signal.

To extract the dipole−dipole paramagnetic contribution from the experimental values, the diamagnetic contribution should be known. To obtain an estimate of the diamagnetic contribution to relaxation, all relaxation rates for each different class of nuclei (Cα, CO, Cβ) were examined, and for each class, the rates of the half with the smallest values were pooled and averaged. These values correspond to nuclei which safely do not experience paramagnetic contributions, as later confirmed from
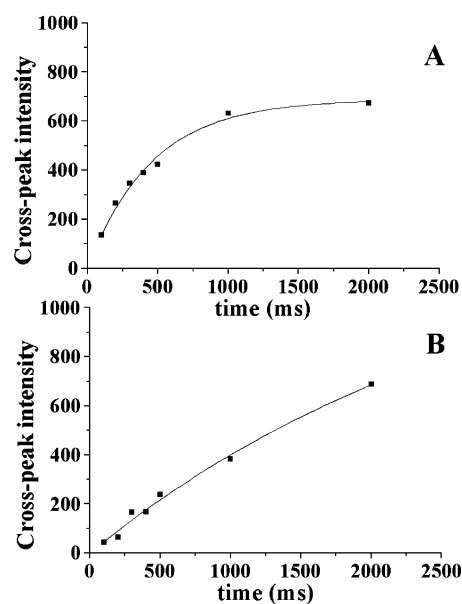
(33) Huffman, D. L.; Huyett, J.; Outten, F. W.; Doan, P. E.; Finney, L. A.; Hoffman, B. M.; O'Halloran, T. V. *Biochemistry* **2002**, *41*, 10046−10055.
(34) Bertini, I.; Luchinat, C.; Rosato, A. *Prog. Biophys. Mol. Biol.* **1996**, *66*, 43−80.
(35) Bertini, I.; Couture, M. M. J.; Donaire, A.; Eltis, L. D.; Felli, I. C.; Luchinat, C.; Piccioli, M.; Rosato, A. *Eur. J. Biochem.* **1996**, *241*, 440−452.
(36) Bertini, I.; Donaire, A.; Luchinat, C.; Rosato, A. *Proteins: Struct., Funct., Genet.* **1997**, *29*, 348−358.
(37) Bertini, I.; Donaire, A.; Felli, I. C.; Luchinat, C.; Rosato, A. *Inorg. Chem.* **1997**, *36*, 4798−4803.

Figure 5. Two SR profiles of ^{13}C−^{13}C CT-COSY spectra and their fittings as an example of "paramagnetic" (A) and "diamagnetic" (B) carbonyl signals.

structure calculations to be far from the metal site. Of the remaining 50% relaxation rates, only those exceeding the diamagnetic average (ρ^{dia}) by more than 10% were considered affected by the paramagnetic center, and the difference taken as paramagnetic relaxation enhancement, ρ^{para}. The latter has been related to the distance from the paramagnetic center through the following relationship:

$$\rho^{para} = k/r_M{}^6$$

where k is a proportionality constant that can be deduced from the constants in the first term of eq 1 using the τ_c of 2 ns determined as discussed previously. The constraints determined with this procedure are reported in Table 1. Only Cα and CO ρ^{para} values were ultimately used as structural constraints, as Cβ ρ^{para} can be affected by local mobility in a more dramatic way than backbone nuclei, thus influencing the precision of the data. As reported in Table 1, and based on the estimated error in the ρ^{para} values, both upper (+15%) and lower (−15%) limits were included in structure calculations.

The 2D and 3D NOESY spectra provide 1777 NOEs which correspond to 1276 meaningful ^{1}H−^{1}H distances, that is, about 200 less than the number of distance constraints used in the structure calculations of apoCopC. The largest differences in the number of NOEs per residue between apo- and Cu(II)-CopC are of course observed for residues localized in the region affected by copper binding and which therefore should constitute the Cu(II) binding site. Additional constraints were provided by 123 dihedral angles and 27 hydrogen bonds.

Paramagnetism-based constraints were constituted by 23 metal−heteronucleus distances, obtained from longitudinal ^{13}C relaxation rates, and by 83 proton pseudocontact shifts. All these constraints were used in the program PSEUDYANA to calculate the solution structure of the Cu(II)-CopC protein. A 35 conformer family of Cu(II)-CopC is shown in Figure 6. The target function is 0.56 ± 0.07 Å^2, and the RMSD values to the mean are 1.07 ± 0.27 Å and 1.58 ± 0.32 Å for backbone and all heavy atoms, respectively. The RMSD of the copper ion,
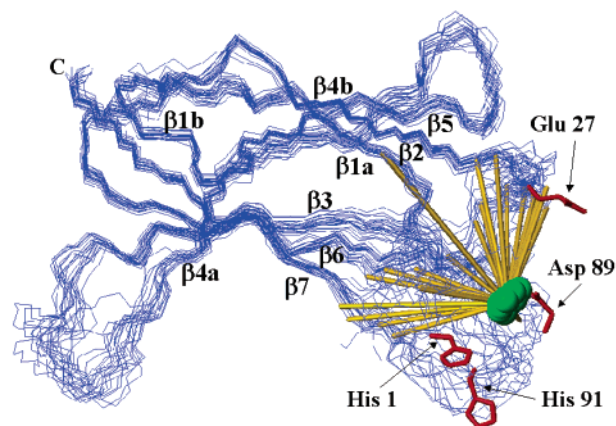
Figure 6. Structure family of Cu(II)-CopC obtained using NMR derived constraints, without applying any link between the residues and the copper ion, which is shown in green. The potential ligands are shown in red. Metal–nucleus distance constraints derived from ^{13}C paramagnetic longitudinal relaxation rate enhancements are shown as yellow bars.

which is only determined by the paramagnetism based constraints, is 1.1 Å. It is immediately apparent that ^{13}C longitudinal relaxation rates are very efficient in determining the position of the copper ion in the protein frame. The metal ion is located in a position equidistant from the loops connecting strands $\beta2$ and $\beta3$ and strands $\beta6$ and $\beta7$ (Figure 6).

This structure family is the result of experimental constraints and is deposited in the PDB (PDB ID code 1OT4).

Hints to Describe the Cu(II) Binding Site. As mentioned previously, there are three residues (His 1, Asp 89, and His 91) for which no information is available from NMR data. From the structural model described previously, these residues are all located at the one end of the molecule which comprises the N-terminal domain (His 1), the loop between strands $\beta2$ and $\beta3$, and the loop between strands $\beta6$ and $\beta7$ (Asp 89 and His 91). These three residues are obvious candidates as metal binding residues. EXAFS data provide additional information in this respect.[20] The Cu(II) ion appears to be bound to two His at 1.99 Å and two other O/N ligands at 1.97 Å, probably in a tetragonal arrangement. Addition of further semicoordinated axial O/N ligand(s) improves the fit of the spectrum.[20] The presence of two histidines is univocal, due to the clear backscattering pattern from the distal ring carbons. Therefore, EXAFS data together with the structural model of Cu(II)-CopC calculated without any metal–ligand constraint clearly indicate His 1 and His 91 as metal ligands. $^{1}H^{-15}N$ HSQC tailored for the detection of ^{2}J $^{1}H^{-15}N$ couplings of nonexchangeable His ring protons confirm that signals belonging to His 1 and 91 are lost, while the signals of the other two His residues of CopC (His 24 and 48) are present with the same chemical shift of the apo protein.

On this basis, we have performed structure calculations by linking the rings of His 1 and 91 to the copper ion. As there is no indication of Nδ or Nϵ coordination, we have linked copper with respect to the center of the His ring. Actually, the system is so little constrained that calculations with Nδ or Nϵ coordination do not allow us to choose between the two binding modes. To link copper to the center of the His ring, we have created a new His residue in the PSEUDODYANA library which contains three additional pseudoatoms, that is, one (QN) in the geometric center of the ring and two (QN1 and QN2) on

opposite sides of the His plane at a distance of 4 Å from QN and lying on the line orthogonal to the ring and passing through its center. Then, we have linked QN of His 1 and 91 to the copper atom through upper and lower limits of 3.4 and 3 Å, respectively, and we have added two lower limits between copper and Hϵ1 and Hδ2 of His. Finally, to ensure that copper lies in the His plane, we have imposed two lower limits of 5 Å between the copper and both QN1 and QN2.

Calculations give rise to a new family of structures of Cu-(II)-CopC with slightly decreased RMSD (0.95 ± 0.17 Å for backbone and 1.40 ± 0.24 Å for heavy atoms) and without an appreciable increase in the target function (0.62 ± 0.06 Å^2). The constraints ensure a correct positioning of the metal with respect to the histidine rings. It appears that both His 1 and 91 are able to coordinate the copper atom either through Nδ or through Nϵ, without any strong preference among the four possible combinations.

The two other ligands are probably oxygen atoms from the carboxylate groups of Asp or Glu residues, in view of the quite short coordination distance found through EXAFS. Besides Asp 89, from the calculated structures, it appears that another conserved residue, that is, Glu 27, whose Cα and side chain nuclei could not be detected (Figure 3B), can be very close to the copper atom. Although unlikely, the side chain nitrogen of Lys 3 could also act as a ligand, because of its missing side chain carbon signals, provided it is deprotonated. Lys 3 is conserved, in a subgroup of proteins with high identity to *P. syringae* CopC.[19] In the apoCopC structure, Lys 3 points toward the interior of the protein and is very close to Glu 27, with which can form a salt bridge.[19] In the present model, due to the lack of constraints, the side chain of Lys is very disordered. Metal coordination might in principle lower the pK_a of a lysine by a few units. However, lowering the pH of Cu(II)-CopC solutions between pH 8.5 and 5.0 does not cause any chemical shift change around Lys 3, whereas, for example, sizable chemical shift changes are seen around other imidazole residues. If we hypothesize that Lys 3 is coordinated to Cu(II) at pH 8.5, it is very unlikely that it remains coordinated down to pH 5.0. Therefore, coordination of Lys 3 in our experimental conditions (pH 7) can be ruled out.

Carboxylate groups of Glu 27 and Asp 89 were then linked to the metal ion through upper and lower distance limits of 2.2 Å and 1.8 Å with one of the two oxygen atoms. This approach does not impose any fixed orientation of the ligands with respect to the copper ion. The structure calculated with these four ligands linked to the metal ion has a target function of 0.85 ± 0.09 Å^2 and RMSD values, to the mean structure, of 0.88 ± 0.20 Å and 1.30 ± 0.28 Å for backbone and all heavy atoms, respectively. The agreement between the observed and calculated ^{1}H pcs's is also good, and the values of axial and rhombic magnetic susceptibility anisotropies converge after two cycles of calculations. The four donor atoms to the copper coordination site form a roughly square planar geometry with the two His in cis positions to one another. It should be stressed that the resulting approximately planar geometry is not originated by any imposed constraints for donor–metal–donor angles. The orientation of the z-axis of the magnetic susceptibility tensor is nearly orthogonal to the ideal plane formed by the donor atoms (see Figure 7), consistent with our structural model.

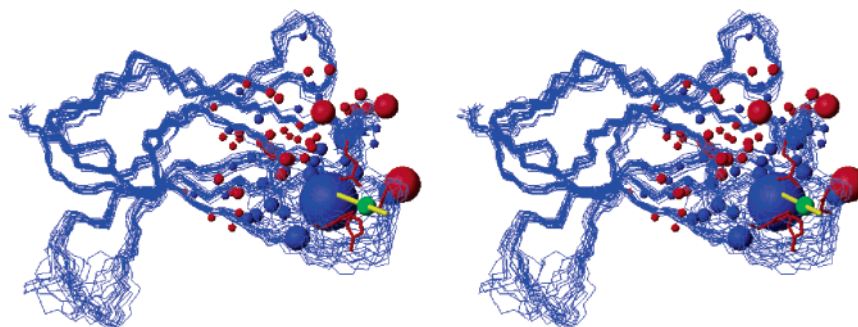The tensor obtained on the last structure can then be used to

Figure 7. Stereoview of the Cu(II)-CopC structure family calculated using NMR constraints and information derived from EXAFS data. Pseudocontact shifts are depicted on the protein frame as spheres (positive = blue, negative = red). The radius of each sphere is proportional to the absolute value of the pseudocontact shift. The principal axis of the magnetic susceptibility tensor is also shown (yellow).

calculate the pcs's of the heteronuclei that are between the 11 Å sphere and the 6 Å sphere. These pcs's are then subtracted from the chemical shift values of Cu(II)-CopC. The resulting chemical shift values have been then compared with the apoCopC values. A few residues very close to copper (roughly less than 8Å distance) experience significant shift differences (0.5–1 ppm) that cannot be ascribed to errors in evaluating their pseudocontact shift, but they most likely originate from structural variations. Differences of this extent are also found for other proteins between the metal bound and metal free forms (for example, Cu(I),Zn(II)-SOD[38] and Zn(II)-SOD[39]), indicating that structural and/or charge changes are occurring upon metal binding which are reflected in changes of the diamagnetic shifts. For this reason, we only rely on ^{13}C pcs's of nuclei located further than 8Å from the metal ion. This leads to 18 further pcs constraints which have been then used in structure calculations.

In the present structural model of Cu(II)-CopC, the Cu(II) binding site lies on a solvent exposed region of the protein. Indeed, NMRD measurements indicate that a water molecule interacts with Cu(II) with a metal–water proton distance of 3.4 Å, corresponding to a metal–oxygen distance of about 2.8 Å. Therefore, a water molecule was linked to the copper ion at a Cu–O distance of 2.8 Å. Lys 3 might be also a candidate for a second weak axial ligand on the less exposed side of the tetragonal plane. However, a weak coordination would lower its pK_a even less than for equatorial coordination, inconsistent with the experimental observation. Lys 3 might still point toward the metal ion, and form a hydrogen bond to one of the two carboxylate donors. This would introduce a positive charge in the metal binding region, which would be otherwise neutral. This positive charge might be functional in determining the reduction potential of the metal thus affecting the redox processes involved in the trafficking of copper in the periplasmic space.

The family of structures calculated with all the constraints discussed previously is characterized by RMSD values of 0.88 ± 0.20 Å and 1.29 ± 0.27 Å for backbone and all heavy atoms, respectively, and a final target function of 0.79 ± 0.09 Å^2. The inclusion of the additional set of pcs's originating from ^{13}C nuclei does not affect the parameters of the χ tensor.

In this structure, the copper site is relatively well-defined as a result of the inclusion of different types of constraints. In addition to four strong ligands located in a square plane, the
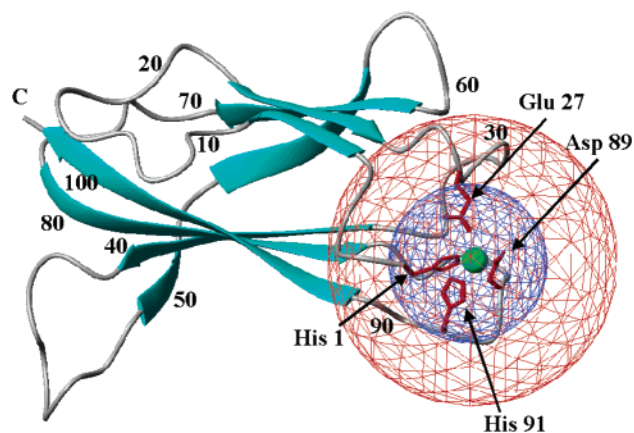

Figure 8. Detection limits through NMR are shown as concentric spheres centered on the copper ion in the Cu(II)-CopC structure calculated applying a link between the copper ion and its potential ligands. The red sphere represents the region in which we are blind using ^1H detection, while using NMR experiments based only on heteronuclei the blind zone restricts to the blue sphere.

water molecule occupies an apical position on the exposed side of the equatorial plane, the long metal–oxygen distance being nicely consistent with the typical semicoordination of axial ligands in tetragonal Cu(II) complexes.[40]

Discussion

Structural studies on Cu(II) binding proteins are challenging due to the paramagnetic nature of the metal ion and its effect on nuclear relaxation of neighboring nuclei. As the interaction between the nuclear spin and the unpaired electron spin on the paramagnetic metal ion is essentially dipolar, the effect on signal line width depends on the reciprocal of the sixth power of the nucleus–metal ion distance.[4] No ^1H signals can be detected inside a sphere of about 11 Å centered on copper, but, when $^{13}C,^{15}N$-tailored experiments are exploited, this detection limit is reduced to a sphere of about 6 Å radius (see Figure 8).

Assignment of a considerable number of signals in the proximity of the paramagnetic center allowed us to move forward and to devise novel structural constraints involving heteronuclei. Out of the large pool of additional structural constraints that can arise from the presence of a paramagnetic center (T$_1$'s,[34–37] pcs,[41–44] residual dipolar couplings arising

(38) Banci, L.; Benedetto, M.; Bertini, I.; Del Conte, R.; Piccioli, M.; Viezzoli, M. S. *Biochemistry* **1998**, *37*, 11780–11791.
(39) Banci, L.; Bertini, I.; Cantini, F.; D'Onofrio, M.; Viezzoli, M. S. *Protein Sci.* **2002**, *11*, 2479–2492.

(40) Cotton, F. A.; Wilkinson, G. *Advanced Inorganic Chemistry*; Wiley: New York, 1990.
(41) Gochin, M.; Roder, H. *Protein Sci.* **1995**, *4*, 296–305.
(42) Banci, L.; Bertini, I.; Gray, H. B.; Luchinat, C.; Reddig, T.; Rosato, A.; Turano, P. *Biochemistry* **1997**, *36*, 9867–9877.

from self-orientation,[44-46] Curie spin/dipole−dipole cross correlated relaxation[44,47]), the most suitable ones in the case of a mildly anisotropic, heavily relaxing paramagnetic metal center such as the type II Cu(II) ion are definitely longitudinal relaxation rate enhancements. Therefore, we focused our attention mainly on this kind of structural constraint and developed a new sequence based on ^{13}C−^{13}C CT-COSY to determine ^{13}C longitudinal relaxation rates and obtain metal−^{13}C distance constraints.

Despite the modest magnetic anisotropy of the paramagnetic copper ion, pcs's could be detected from both ^{1}H and ^{13}C nuclei and also used as constraints.

The structure of Cu(II)-CopC has a global backbone RMSD comparable to that of the diamagnetic forms of the protein.[19,20] The comparison between apo- and Cu(II)-CopC forms, with the latter being relatively well-defined thanks to the new constraints in the proximity of the Cu(II) binding site, indicates that small structural changes are observed only in the region around copper. The solution structure of Cu(I)-CopC showed that the Cu(I) site is constituted by a His and two/three Met residues, which are clustered in a Met-rich region.[20] Both Cu(I) and Cu(II) binding sites represent novel coordination environments for copper in proteins. It was found that copper binds selectively to the two different binding sites, depending on the copper oxidation state.[20] It was also proposed that the redox state of copper bound to CopC acts as a switch between the possible trafficking pathways of the metal ion.[20]

The arrangement of the ligands and the exposed location of the Cu(II) site provide hints on how the Cu(II) ion is transported inside the cell. The prerequisite of kinetic lability of metal binding for metallochaperone proteins is satisfied by the exposed location of the metal binding motif, which favors the formation, in the complex, of metal bridged intermediates between the metal donor and the metal acceptor proteins and allows a fast and efficient metal uptake and release mechanism without significant structural rearrangements.

Recent studies have shown that, in the case of paramagnetic metalloproteins, the metal binding site can be modeled on similar sites already structurally characterized.[48] However, a reliable template structure is not always available, particularly when the metal ion is bound to an exposed metal binding site. In the specific case of copper trafficking proteins, crystallization was attempted for the copper bound form, but it did not provide good structural models for the physiologically relevant state.[49] Some successful attempts used non-native metal ions (i.e., Hg-(II) and Ag(I)).[50] Therefore, modeling the metal site on known structural models might not be a general strategy.

We have here developed an approach which allows a further major step in the structure determination of paramagnetic metalloproteins with unfavorable relaxation properties. Not only have we expanded signal detection and spectral assignment but also translated this info in a source of structural constraints. Furthermore, we have analyzed and used in a strategic way these constraints, depending on their correlation with the metal ion and on their sensitivity to paramagnetic effects. Finally, the inclusion of EXAFS data in the solution structure calculations can provide complementary information on the metal site, which can constitute a general strategy in the structure determination of metalloproteins.

The difficulties in solution structure determination of paramagnetic metalloproteins underscore the importance of the present study which represents the first example of an NMR structural characterization of a protein having a type II copper site. The protein CopC is also the first characterized Cu(II) binding protein involved in copper trafficking, which opens new scenarios in the overall copper homeostasis process.

Supporting Information Available: Table of ^{15}N and ^{13}C resonance assignments of Cu(II)-CopC at 298 K, pH 7.0, in water solution. This material is available free of charge via the Internet at http://pubs.acs.org.

JA034112C

(43) Arnesano, F.; Banci, L.; Bertini, I.; Felli, I. C. *Biochemistry* **1998**, *37*, 173−184.
(44) Hus, J. C.; Marion, D.; Blackledge, M. *J. Mol. Biol.* **2000**, *298*, 927−936.
(45) Bertini, I.; Janik, M. B. L.; Liu, G.; Luchinat, C.; Rosato, A. *J. Magn. Reson.* **2001**, *148*, 23−30.
(46) Barbieri, R.; Bertini, I.; Cavallaro, G.; Lee, Y. M.; Luchinat, C.; Rosato, A. *J. Am. Chem. Soc.* **2002**, *124*, 5581−5587.
(47) Bertini, I.; Cavallaro, G.; Cosenza, M.; Kummerle, R.; Luchinat, C.; Piccioli, M.; Poggi, L. *J. Biomol. NMR* **2002**, *23*, 115−125.
(48) Pochapsky, T. C.; Pochapsky, S. S.; Ju, T.; Mo, H.; Al-Mjeni, F.; Maroney, M. J. *Nat. Struct. Biol.* **2002**, *9*, 966−972.
(49) Wernimont, A. K.; Huffman, D. L.; Lamb, A. L.; O'Halloran, T. V.; Rosenzweig, A. C. *Nat. Struct. Biol.* **2000**, *7*, 766−771.
(50) Rosenzweig, A. C.; Huffman, D. L.; Hou, M. Y.; Wernimont, A. K.; Pufahl, R. A.; O'Halloran, T. V. *Structure Fold Des.* **1999**, *7*, 605−617.
(51) In principle, also contact contributions to relaxation might be reduced by a lower γ, but as unpaired spin delocalization on ligand nuclei is usually much stronger for ^{13}C and ^{15}N nuclei than for ^{1}H, this gain is very limited. In any case, the majority of ^{13}C and ^{15}N nuclei, with the exception of copper-coordinating residues, are not expected to experience sizable Fermi contact relaxation.